研究简报

钐-邻硝基苯甲酸与 1,10-邻菲咯啉配合物的热分解动力学

任 宁[1,3] 张建军*[,1,2] 张存英[4] 宿素玲[1,2] 张海燕[1,2] 田 靓[1,2]
([1]河北师范大学实验中心,石家庄 050016)
([2]河北师范大学化学与材料科学学院,石家庄 050016)
([3]邯郸学院化学系,邯郸 056005)
([4]石家庄市第一中学,石家庄 050011)

关键词: 邻硝基苯甲酸; 1,10-邻菲咯啉; 钐配合物; 热分解动力学
中图分类号: O643.12 **文献标识码**: A **文章编号**: 1001-4861(2007)06-1078-07

Thermal Decomposition Kinetics of Sm(Ⅲ) Complex with *o*-Nitrobenzoate and 1,10-phenanthroline

REN Ning[1,3] ZHANG Jian-Jun*[,1,2] ZHANG Cun-Ying[4] XU Su-Ling[1,2] ZHANG Hai-Yan[1,2] TIAN Liang[1,2]
([1]*Experimental Center, Hebei Normal University, Shijiazhuang* 050016)
([2]*Chemistry & Material Science, Hebei Normal University, Shijiazhuang* 050016)
([3]*Department of Chemistry, Handan College, Handan, Hebei* 056005)
([4]*No.*1 *High School of Shijiazhuang, Shijiazhuang* 050011)

Abstract: The complex of $Sm_2(o\text{-NBA})_6(PHEN)_2$ (*o*-NBA, *o*-Nitrobenzoate; PHEN, 1,10-phenanthroline) was prepared and characterized by elemental analysis, IR and UV spectraoscopy. The thermal decomposition mechanism of $Sm_2(o\text{-NBA})_6(PHEN)_2$ was studied under a static air atmosphere by TG-DTG. The thermal decomposition kinetics of the complex for the first stage was studied under non-isothermal condition. The most probable mechanism functions of the thermal decomposition reaction for the first stage are: $G(\alpha)=[-\ln(1-\alpha)]^{1/2}$, $f(\alpha)=2(1-\alpha)[-\ln(1-\alpha)]^{1/2}$. The activation energy E for the first stage is 259.50 kJ·mol^{-1}, the pre-exponential factor A is 36.19×10^{18} min^{-1}. The lifetime equation at weight-loss of 10% was deduced as $\ln\tau=-36.70+27\,572.12/T$ by isothermal thermogravimetric analysis.

Key words: *o*-Nitrobenzoic acid; 1,10-phenanthroline; samarium complex; thermal decomposition kinetics

Rare earth mixed-ligands carboxylate complexes containing 1,10-phenanthroline have been extensively investigated[1-6], because of their special structures and interesting luminous properties. They can be used in many areas such as extraction and separation, germicide, catalyst, luminous materials, functional materials and so on. In our previous studies[7-14], we reported the preparation, crystal structure and thermal decomposition mechanism of a number of ternary lanthanide complexes of benzoic acid or its derivatives with 1,10-phenanthroline. In this paper, we report the synthesis of a new samarium complex using the mixed-

收稿日期:2007-03-15。收修改稿日期:2007-04-10。
河北省自然科学基金(No.B2007000237),河北省教育厅自然科学基金(No.2004325)及河北师范大学重点自然科学基金(No.L2006Z06,L2005Y12)资助项目。
*通讯联系人。E-mail:jjzhang6@126.com
第一作者:任 宁,女,27 岁,硕士研究生;研究方向:配位化学及热分析动力学。

ligands of *o*-nitrobenzoic acid and 1,10-phenanthroline. The thermal decomposition mechanism for the complex was studied by TG-DTG, and the non-isothermal kinetics was discussed using the literature reported method[15,16]. The knowledge of the thermodynamic properties of the complex is important to help the understanding of the structure itself, and to characterize and understand the properties of the coordination compound, which eventually could be useful in determining their potential applications.

1 Experimental

1.1 Materials

All regents used were Analytical grade and were used without further purification.

1.2 Synthesis of complex $Sm_2(o\text{-}NBA)_6(PHEN)_2$

$SmCl_3\cdot 6H_2O$, *o*-NBA and PHEN were dissolved in 95% ethanol, respectively, in a molar ratio of 1∶3∶1. The pH value of the *o*-NBA was adjusted to 6~7 by adding 1.0 mol L^{-1} NaOH solution. The ethanol solution of the two ligands was mixed and then added dropwise to the ethanolic $SmCl_3$ solution. At once a large white precipitate formed. The mixture solution was stirred for 8 h at room temperature and then deposited for 12 h. Subsequently, the precipitate was filtered out and washed three times with deionized water and 95% ethanol. The white powdery complex $Sm_2(o\text{-}NBA)_6(PHEN)_2$ was obtained with a yield of 85%.

1.3 Chacterization

The contents of carbon, hydrogen and nitrogen were determined by elemental analysis using a Carlo-Erba model 1106 elemental analyzer. The metal content was assayed using EDTA titration method. Infrared spectra were recorded over the range 4 000~400 cm^{-1}, using Perkin-Elmer 1730 FTIR spectrometer as KBr discs. UV spectra were depicted on SHIMADZU 2501 spectrometer. The TG and DTG curves were obtained under air atmosphere with a Perkin Elmer′s TGA7 thermogravimetric analyzer. The heating rates were 3, 5, 7, 10, 12 $K\cdot min^{-1}$ from ambient to 950 ℃ and the sample size was 2.3±0.2 mg.

1.4 Methodology and kinetic analysis

The procedure for data processing of thermal analysis kinetics are as follows[15,16].

1.4.1 Determination of the function of conversion

Flynn-Wall-Ozawa equation[17] is as follows:

$$\lg\beta=\lg\left(\frac{AE}{RG(\alpha)}\right)-2.315-0.456\,7\frac{E}{RT} \quad (\mathbf{1})$$

Eq.(**1**) is changed into:

$$\lg G(\alpha)=\lg\left(\frac{AE}{R}\right)-2.315-0.456\,7\frac{E}{RT}-\lg\beta \quad (\mathbf{2})$$

where $G(\alpha)$ is the integral mechanism function, T the absolute temperature, A the pre-exponential factor, R the gas constant, E the apparent activation energy and β the linear heating rate.

On substitution the values of conversion degrees at the same temperature on several TG curves, the different mechanism functions $G(\alpha)$ and various heating rates into Eq.(**2**), the linear correlation coefficient r, the slope b and the intercept a at different temperatures are obtained by the linear least square method with $\lg G(\alpha)$ vs $\lg\beta$. If the linear correlation coefficient r is the best and the slope b approaches −1. The relevant function is the probable mechanism function of a solid phase reaction. The common mechanism functions in non-isothermal reaction kinetics are listed in Table 1[18].

Table 1　Forty types of kinetic mechanism functions[18]

Mechanism (code)	Name of function	Mechanism	Form of function	
			$G(\alpha)$	$f(\alpha)$
1	Parabola law	One-dimensional diffusion, 1D	α^2	$1/2\alpha^{-1}$
2	Valensi equation	Two-dimensional diffusion, 2D	$\alpha+(1-\alpha)\ln(1-\alpha)$	$[-\ln(1-\alpha)]^{-1}$
3	Jander equation	Two-dimensional diffusion 2D, n=1/2	$[1-(1-\alpha)^{1/2}]^{1/2}$	$4(1-\alpha)^{1/2}[1-(1-\alpha)^{1/2}]^{1/2}$
4	Jander equation	Two-dimensional diffusion 2D, n=2	$[1-(1-\alpha)^{1/2}]^2$	$(1-\alpha)^{1/2}[1-(1-\alpha)^{1/2}]^{-1}$
5	Jander equation	Two-dimensional diffusion 3D, n=1/2	$[1-(1-\alpha)^{1/3}]^{1/2}$	$6(1-\alpha)^{2/3}[1-(1-\alpha)^{1/3}]^{1/2}$
6	Jander equation	Three-dimensional diffusion 3D, n=2	$[1-(1-\alpha)^{1/3}]^2$	$3/2[1-(1-\alpha)^{1/3}]^{1/2}$
7	G.-B equation	Three-dimensional diffusion 3D, D_4	$1-2\alpha/3-(1-\alpha)^{2/3}$	$3/2[(1-\alpha)^{-1/3}-1]^{-1}$

Continued Table 1

8	Anti-Jander equation	Three-dimensional diffusion 3D	$[(1+\alpha)^{1/3}-1]^2$	$3/2(1+\alpha)^{2/3}[(1+\alpha)^{1/3}-1]^{-1}$
9	Z.-L.-T. equation	Three-dimensional diffusion 3D	$[(1-\alpha)^{-1/3}-1]^2$	$3/2(1-\alpha)^{4/3}[(1-\alpha)^{-1/3}-1]^{-1}$
10	Avrami-Erofeev	Nucleation and growth, n=1/4, m=4	$[-\ln(1-\alpha)]^{1/4}$	$4(1-\alpha)[-\ln(1-\alpha)]^{3/4}$
11	Avrami-Erofeev	Nucleation and growth, n=1/3, m=3	$[-\ln(1-\alpha)]^{1/3}$	$3(1-\alpha)[-\ln(1-\alpha)]^{2/3}$
12	Avrami-Erofeev	Nucleation and growth, n=2/5	$[-\ln(1-\alpha)]^{2/5}$	$2/5(1-\alpha)[-\ln(1-\alpha)]^{3/5}$
13	Avrami-Erofeev	Nucleation and growth, n=1/2, m=2	$[-\ln(1-\alpha)]^{1/2}$	$2\ (1-\alpha)[-\ln(1-\alpha)]^{1/2}$
14	Avrami-Erofeev	Nucleation and growth, n=2/3	$[-\ln(1-\alpha)]^{2/3}$	$3/2(1-\alpha)[-\ln(1-\alpha)]^{1/3}$
15	Avrami-Erofeev	Nucleation and growth, n=3/4	$[-\ln(1-\alpha)]^{3/4}$	$4/3(1-\alpha)[-\ln(1-\alpha)]^{1/4}$
16	Avrami-Erofeev	Nucleation and growth, n=1, m=4	$-\ln(1-\alpha)$	$(1-\alpha)$
17	Avrami-Erofeev	Nucleation and growth, n=3/2	$[-\ln(1-\alpha)]^{3/2}$	$2/3(1-\alpha)[-\ln(1-\alpha)]^{-1/2}$
18	Avrami-Erofeev	Nucleation and growth, n=2	$[-\ln(1-\alpha)]^2$	$1/2(1-\alpha)[-\ln(1-\alpha)]^{-1}$
19	Avrami-Erofeev	Nucleation and growth, n=3	$[-\ln(1-\alpha)]^3$	$1/3(1-\alpha)[-\ln(1-\alpha)]^{-2}$
20	Avrami-Erofeev	Nucleation and growth, n=4	$[-\ln(1-\alpha)]^4$	$1/4(1-\alpha)[-\ln(1-\alpha)]^{-3}$
21	P.-T. equation	Autocatalysis	$\ln[\alpha/(1-\alpha)]$	$\alpha(1-\alpha)$
22	Mampel Power law	n=1/4	$\alpha^{1/4}$	$4\alpha^{3/4}$
23	Mampel Power law	n=1/3	$\alpha^{1/3}$	$3\alpha^{2/3}$
24	Mampel Power law	n=1/2	$\alpha^{1/2}$	$2\alpha^{1/2}$
25	Mampel Power law	n=1	α	1
26	Mampel Power law	n=3/2	$\alpha^{3/2}$	$2/3\alpha^{-1/2}$
27	Mampel Power law	n=2	α^2	$1/2\alpha^{-1}$
28	Reaction order	n=1/4	$1-(1-\alpha)^{1/4}$	$4(1-\alpha)^{3/4}$
29	Contracting sphere (volume)	Phase boundary reaction, n=1/3	$1-(1-\alpha)^{1/3}$	$3(1-\alpha)^{2/3}$
30		n=3 (three dimensional)	$3[1-(1-\alpha)^{1/3}]$	$(1-\alpha)^{2/3}$
31	Contracting cylinder (area)	Phase boundary reaction, n=1/2	$1-(1-\alpha)^{1/2}$	$2(1-\alpha)^{1/2}$
32	Reaction order	n=2	$1-(1-\alpha)^2$	$1/2(1-\alpha)^{-1}$
33	Reaction order	n=3	$1-(1-\alpha)^3$	$1/3(1-\alpha)^{-2}$
34	Reaction order	n=4	$1-(1-\alpha)^4$	$1/4(1-\alpha)^{-3}$
35	Second order	Chemical reaction, F_2	$(1-\alpha)^{-1}$	$(1-\alpha)^2$
36	Reaction order	Chemical reaction	$(1-\alpha)^{-1}-1$	$(1-\alpha)^2$
37	Two thirds order	Chemical reaction	$(1-\alpha)^{-1/2}$	$2(1-\alpha)^{3/2}$
38	Exponent law	E_1, n=1	$\ln\alpha$	α
39	Exponent law	n=2	$\ln\alpha^2$	$1/2\alpha$
40	Third order	Chemical reaction, F_3	$(1-\alpha)^{-2}$	$(1-\alpha)^{3/2}$

1.4.2 Calculation of E and A

By substituting the values of temperatures at the same degree of conversion, heating rates and the conversion function $G(\alpha)$ determined above in Eq.(**1**), the linear correlation coefficient r, the slope b and the intercept a at the different conversion degrees are obtained by the linear least square method with $\lg\beta$ vs $1/T$. From the value of the slope for the plot, E can be calculated. From the value of the intercept, A can be also calculated.

2 Results and discussion

2.1 Elemental analysis

The analysis data of the element content are shown in Table 2. It can be seen that the experimental data are

Table 2 Elemental analysis data of [Sm(*o*-NBA)$_3$PHEN]$_2$(%)

Complex [Sm(*o*-NBA)$_3$PHEN]$_2$	Mass fraction / %			
	C	H	N	Sm
Found	47.60	2.52	8.43	18.06
Theoretical	47.76	2.77	8.44	18.14

in good agreement with the theoretical values.

2.2 Infrared spectra

The band at 1 682 cm^{-1} originating from the COOH group for free acid ligand, completely disappeared in the spectra of the complex. However, the asymmetric and symmetric vibrations of the COO^- group at 1 573 cm^{-1} and 1 403 cm^{-1} are present in the spectra of the complex, which indicates that the oxygen in the carboxylate group are coordinated to Sm(Ⅲ)[19]. The bands of $\nu_{C=N}$ (1 646 cm^{-1}) and δ_{C-H} (854 cm^{-1}, 740 cm^{-1}) in the spectra of 1,10-phenanthroline ligand, shift to 1 618, 845 and 731 cm^{-1} in the spectra of the complex, respectively, and this may suggest the coordination of two nitrogen atoms of the 1,10-phenanthroline to Sm^{3+}ion[20].

2.3 UV spectra

The complex and ligands have strong $\pi \rightarrow \pi^*$ transition absorption. There is a strong absorption band at 253 cm^{-1} in the *o*-nitrobenzoic acid ligand, which shifts to longer wavelength of 264.00 nm in the complex. The fact may be explained by the π-conjugated system caused by the metal coordination[21]. The maximum absorption wavelength of the complex is very similar to that observed from the 1,10-phenanthroline ligand, suggesting that the formation of the Sm-N has no conspicuous effect on the UV absorption of the 1,10-phenanthroline.

2.4 Thermal decomposition mechanism

The TG-DTG curves of the title complex at a heating rate of 5 $K \cdot min^{-1}$ in static air atmosphere are presented in Fig.1. The process can be divided into two stages as shown in the DTG curve. The first decomposition process starts from 306.85 ℃ to 421.04 ℃ with a mass loss of 47.14%. The degradation can be explained by the bond lengths. The mental-N distance is longer than other bond distances [14]. Theoretically, this bond is less stable and easy to be broken down. In addition, The IR spectra of the residue at 421.04 ℃ shows the disappearance of the absorption band of C=N at 1 618 cm^{-1}. So, 2 mol PHEN is lost early in the first decomposition process. But, theoretical loss of 2 mol PHEN is 21.74%, which is lower than the weight loss (47.14%) observed, indicating that the part of *o*-NBA ligands have also been lost.

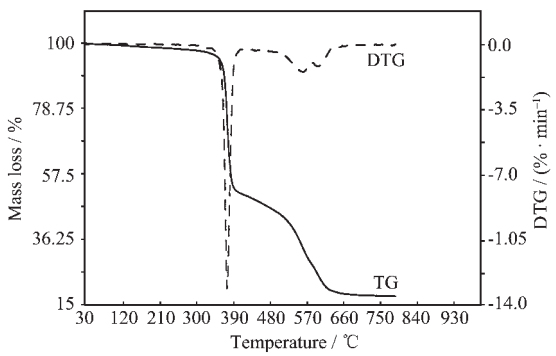

Fig.1　TG-DTG curves of $[Sm(o\text{-}NBA)_3PHEN]_2$ (β=5 ℃·min^{-1})

It is in two steps that the remainder *o*-NBA ligands are lost. It begins at 421.04 ℃ and ends at 655.18 ℃ with a mass loss of 31.65%. Up to 655.18 ℃, the spectrum of the residue is consistent with the standard spectrum of Sm_2O_3. Therefore, the title complex is completely degraded into Sm_2O_3 (observed, 21.10%; calculated, 21.03%).

2.5 Kinetics of the first decomposition stage

2.5.1 Determination of $f(\alpha)$ and $G(\alpha)$

The values of conversion degrees at the same temperature on five TG curves of the title complex are listed in Table 3. By substituting the values of α, β in Table 3 and various conversion functions $G(\alpha)$ in Table 1 into Eq.(**2**), the linear correlation coefficient *r*,

Table 3　Conversion degrees measured for given temperature on the TG-DTG curves of $[Sm(o\text{-}NBA)_3PHEN]_2$ at different heating rates: Stage Ⅰ

T / K	α				
	β=3 K·min^{-1}	β=5 K·min^{-1}	β=7 K·min^{-1}	β=10 K·min^{-1}	β=12 K·min^{-1}
645.60	0.578 25	0.384 76	0.192 32	0.092 35	0.063 36
646.93	0.639 88	0.446 06	0.251 07	0.116 77	0.078 68
648.26	0.719 37	0.540 68	0.297 13	0.135 77	0.091 41
657.35	—	0.873 52	0.744 28	0.467 68	0.311 69
660.68	—	—	0.848 89	0.635 51	0.459 04

the slope b and the intercept a at the different temperatures were obtained by the linear least square method with $\lg G(\alpha)$ vs $\lg\beta$. Part of results are listed in Table 4.

From Table 4, it can be easily seen that only the coefficients r of the function No.13 is the best and the slope b approaches −1, so the probable mechanism function is $G(\alpha)=[-\ln(1-\alpha)]^{1/2}$, $f(\alpha)=2(1-\alpha)[-\ln(1-\alpha)]^{1/2}$.

2.5.2 Calculation of E and A

The values of temperatures at the same degree of conversion on five TG curves of the title complex are listed in Table 5.

By substituting the values of α, β, T in Table 5 and conversion function into Eq. (**1**), the linear correlation coefficient r, the slope b and the intercept a at the different conversion degrees are obtained by

Table 4 Part of the results from the linear least squares method at different temperatures for[Sm(*o*-NBA)$_3$PHEN]$_2$: Stage Ⅰ

T / K	Function No.	a	b	r
	5	0.172 36	−0.911 81	−0.987 2
645.60	13	0.462 45	−0.959 68	−0.989 4
	14	0.616 60	−1.279 52	−0.989 3
	13	0.489 63	−0.932 49	−0.986 5
646.93	14	0.652 84	−1.243 35	−0.986 5
	40	−0.669 19	1.289 05	0.998 1
	13	0.559 30	−0.963 93	−0.982 8
648.26	14	0.745 73	−1.285 24	−0.982 7
	40	−0.903 32	1.485 60	0.996 0
	13	0.860 52	−0.974 54	−0.987 3
657.35	14	1.147 37	−1.299 39	−0.987 3
	38	1.130 61	−0.982 35	−0.998 2
	13	1.005 51	−1.019 77	−0.993 1
660.68	14	1.340 68	−1.359 69	−0.993 1
	38	1.414 40	−1.190 13	−0.999 4

Table 5 Temperatures corresponding to the same degree of conversion at different heating rates for [Sm(*o*-NBA)$_3$PHEN]$_2$: Stage Ⅰ

α	T / K				
	β=3 K·min^{-1}	β=5 K·min^{-1}	β=7 K·min^{-1}	β=10 K·min^{-1}	β=12 K·min^{-1}
0.1	630.80	635.24	640.95	646.19	648.93
0.15	635.24	639.01	643.83	649.07	651.81
0.2	637.90	641.23	645.60	651.07	653.80
0.25	639.45	642.56	646.93	652.40	655.58
0.3	640.56	643.89	648.26	653.73	656.69
0.35	641.67	645.00	649.15	655.06	658.02
0.4	642.78	646.11	650.26	656.17	659.12
0.45	643.67	647.00	651.14	657.28	660.23
0.5	644.56	647.88	651.81	658.16	661.34
0.55	645.44	648.77	652.92	658.83	662.45
0.6	646.11	649.44	654.03	660.16	663.56
0.65	647.00	650.54	655.14	661.27	664.67
0.7	648.11	651.65	656.24	662.38	666.22
0.75	649.21	653.21	657.35	663.71	667.55
0.8	650.54	654.54	658.68	665.26	669.32

Table 6　Values of the kinetics parameters computed by the Flynn-Wall-Ozawa method for [Sm(*o*-NBA)$_3$PHEN]$_2$: Stage Ⅰ

α	E / (kJ·mol^{-1})	E_a / (kJ·mol^{-1})	$A \times 10^{18}$ / min^{-1}	$A^a \times 10^{18}$ / min^{-1}	r
0.1	237.71		3.81		−0.993 1
0.15	262.29		42.00		−0.989 8
0.2	272.69		30.62		−0.985 3
0.25	270.16		18.95		−0.981 6
0.3	271.96		26.91		−0.984 5
0.35	267.83		12.24		−0.982 2
0.4	268.87	259.50	14.88	36.19	−0.982 2
0.45	265.12		72.92		−0.981 1
0.6	254.50		96.97		−0.980 4
0.65	253.43		78.33		−0.982 3
0.7	249.30		35.20		−0.980 3
0.8	233.72		1.8		−0.989 1

[a] Average value of E, A.

the linear least square method with lgβ vs 1/T. The activation energy E can be calculated from the value of the slope and the pre-exponential factor A can also be calculated from the value of the intercept. The results are listed in Table 6.

2.6　Lifetime

The general lifetime formula of materials is as follows[22]:

$$\ln\tau = a + b/T \qquad (3)$$

where τ is the lifetime at temperature T (K), a and b are constant. In this paper, the mass-loss of 10% lifetime was measured by isothermal temperature TG at 598.15, 608.15, 618.15 and 628.15 K and is listed in Table 7. By substituting the values in Table 7 into equation (**3**), the constant a, b and linear correlation coefficients r are obtained by the linear least square method. The lifetime equation is $\ln\tau = -36.70 + 27\,572.12/T$, the linear correlation coefficients r is 0.990 5.

Table 7　Lifetime of [Sm(*o*-NBA)$_3$PHEN]$_2$ by isothermal temperature TG

T / K	$\tau_{10\%}$ / min	T / K	$\tau_{10\%}$ / min
598.15	185.74	618.15	39.68
608.15	111.44	628.15	22.68

3　Conclusions

The thermal decomposition process of [Sm(*o*-NBA)$_3$PHEN]$_2$ are divided into two steps. The mechanism function of the first-stage decomposition reaction is $G(\alpha)=[-\ln(1-\alpha)]^{1/2}$. The activation energy E is 259.50 kJ·mol^{-1} and the pre-exponential factor A is 36.19×10^{18} min^{-1}. The lifetime equation at mass-loss of 10% is deduced as $\ln\tau = -36.70 + 27\,572.12/T$ by isothermal thermogravimetric analysis.

References:

[1] Jin L P, Wang M Z, Cai G L, et al. *Science in China*(*Series B*), **1995**,**38**:1~9

[2] Jin L P, Wang R F, Li L S. *J. Rare Earths*., **1996**,**14**:161~166

[3] LI Xia(李　夏), REN Gui-Fen(任桂芬), LIU Meng-You(刘孟友), et al. *Guangpuxue Yu Guangpufenxi*(*Spectroscopy and Spectral Analysis*), **2004**,**24**(11):1410~1411

[4] WANG Shao-Ting(王少亭), YANG Yong-li(杨永丽), LI Xia(李　夏). *Guangpuxue Yu Guangpufenxi*(*Spectroscopy and Spectral Analysis*), **2000**,**20**(3):324~325

[5] LI Xia(李　夏), CHU Yi-Ming(初一鸣). *Wuji Huaxue Xuebao* (*Chinese J. Inorg. Chem.*), **2006**,**22**(1):145~148

[6] Niu S Y, Jin J, Jin X L, et al. *Solid State Sciences*, **2002**,**4**: 1103~1106

[7] Ren N, Zhang J J, Xu S L, et al. *Thermochimica Acta*, **2005**, **438**:172~177

[8] Ren N, Zhang J J, Wang R F, et al. *J. Chin. Chem. Soc*., **2006**,**53**(2):293~298

[9] Zhang J J, Ren N, Xu S L. *Chin. J. Chem.*, **2007**,**25**:125~128

[10]Zhang J J, Ren N, Wang Y X, et al. *J. Braz. Chem. Soc*., **2006**,**17**(7):1355~1359

[11]REN Ning(任　宁), ZHANG Jian-Jun(张建军), XU Su-Ling(宿素玲), et al. *Wuji Huaxue Xuebao*(*Chinese J. Inorg. Chem.*), **2006**,**22**(10):1905~1907

[12]Zhang J J, Ren N, Bai J H, Xu S L. *Int. J. Chem. Kinet.*, **2007**,**39**:67~74

[13]Xu S L, Zhang J J, Yang H F, et al. *Z. Naturforsch.*, **2007**, **62b**:51~54

[14]Zhang J J, Wang R F, Zhang J L, et al. *Chem. Res Chinese U.*, **2002**,**18**(1):25~29

[15]REN Ning(任 宁), ZHANG Jian-Jun(张建军). *Huaxue Jinzhan*(*Progress in Chemistry*), **2006**,**18**(4):410~416

[16]Zhang J J, Ren N. *Chin. J. Chem.*, **2004**,**22**:1459~1462

[17]Ozawa T. *Bull. Soc. Chem. Jpn.*, **1965**,**38**:1881~1886

[18]HU Rong-Zu(胡荣祖), SHI Qi-Zhen(史启祯). *Thermal Analysis Kinetics*(热分析动力学). Beijing: Science Press, **2001**. 127

[19]SHI Yao-Ceng(施耀曾), SUN Xiang-Zhen(孙祥祯), JIANG Yan-Hao(蒋燕灏). *Spectra and Chemical Identification of Organic Compounds*(有机化合物光谱和化学鉴定). Nanjing: Science and Technology Press, **1988**.98

[20]BAI Guang-Zhou(白光弼), CHEN Guang-De(陈广德), WANG Zhe-Ming(王喆明), et al. *Wuji Huaxue*(*Chinese J. Inorg. Chem.*), **1988**,**4**:32~41

[21]An B L, Gong M L, Li M X, et al. *J. Mol. Struct.*, **2004**,**687**: 1~6

[22]Zhang J J, Wang R F, Wang S P, et al. *J. Therm. Anal. Cal.*, **2005**,**79**:181~186